This article has been accepted for publication in a future issue of this journal, but has not been fully edited. Content may change prior to final publication. Citation information: DOI 10.1109/ACCESS.2021.3112612, IEEE Access

IEEE Access
Multidisciplinary | Rapid Review | Open Access Journal

A Deep Neural Network Model for Predicting Electric Fields Induced by Transcranial Magnetic Stimulation Coil

Khaleda Akhter Sathi[1], Md. Azad Hossain[1], (Member, IEEE), Md. Kamal Hosain[2], Nguyen Hoang Hai[3], (Member, IEEE), and Md. Anwar Hossain[4], (Senior Member, IEEE)

[1]Department of Electronics and Telecommunication Engineering, Chittagong University of Engineering & Technology, Chattogram 4349, Bangladesh
[2]Department of Electronics & Telecommunication Engineering, Rajshahi University of Engineering & Technology, Rajshahi-6204, Bangladesh
[3]School of Electronics and Telecommunication, Hanoi University of Science and Technology, Thanh Xuan District, Hanoi 100000, Vietnam
[4]Department of Electrical and Electronic Engineering, Bangladesh University of Business and Technology (BUBT), Dhaka-1216, Bangladesh

Corresponding authors: Khaleda Akhter Sathi (sathi.ete@cuet.ac.bd), Md. Azad Hossain (azad@cuet.ac.bd), and Md. Kamal Hosain (khosain@ete.ruet.ac.bd).

ABSTRACT This article proposes a deep neural network (DNN) model to predict the electric field induced by a transcranial magnetic stimulation (TMS) coil under high-amplitude and low-frequency current pulse conditions. The DNN model is comprised of an input layer with 6 neurons, three non-linear hidden layers with a total of 1088 neurons, and a linear single output layer. The model is developed in Google Colaboratory environment with TensorFlow framework using six features including coil turns of single wing, coil thickness, coil diameter, distance between two wings, distance between head and coil position, and angle between two wings of coil as the inputs and electric field as the output. The model performance is evaluated based on four verification statistic metrics such as coefficient of determination (R^2), mean squared error (MSE), mean absolute error (MAE), and root mean squared error (RMSE) between the simulated and predicted values. The proposed model provides an adequate performance with R^2 = 0.766, MSE = 0.184, MAE = 0.262, and RMSE = 0.429 in the testing stage. Therefore, the model can successfully predict the electric field in an assembly TMS coil without the aid of electromagnetic simulation software that suffers from an extensive computational cost.

INDEX TERMS Deep Neural Network, Deep Learning, Electric Field, Magnetic Coil, Transcranial Magnetic Stimulation.

I. INTRODUCTION

Transcranial magnetic stimulation (TMS) has shown an effective therapeutic outcome for some neural disorders such as major depressive disorder, traumatic brain injury, parkinson's disease, post-traumatic stress disorder, etc. [1-4]. The TMS technique requires a magnetic coil normally placed on the subject's head that is fed with a high-valued short-duration current pulse [5]. The electric current conveyed in the coil produces a magnetic field that results in an induced electric field inside the brain tissues [6]. Then a localized axial depolarization is formed by the induced electrical field in the underlying cortical tissue which has a therapeutic effectiveness of neural disorders [7]. To ensure a greater therapeutic effect, the induced electric field should have to be strong enough so that it can depolarize the target neurons that are responsible for the neural disorders [8, 9]. Moreover, some other factors including focality (area of stimulation) and depth (distance from vertex) of the induced electric field are associated with the effectiveness of TMS treatment. The commercially available single coils named as figure-eight, halo, circular, double cone, H, etc. are suffering from the trade-off between stimulation focality and depth. For instance, the figure-eight coil aims to generate a concentrated electric field within a smaller region rather than stimulating the deeper brain structure. Alternatively, the H-coil increases the stimulation depth by maintaining a moderate focality. The Halo coil also stimulates the deep brain structure but it degrades the focality. Thus, in the recent research the development of an assembly coil (combination of single coils) is emphasized to maintain a trade-off between stimulation depth and focality [10].

As the electric field intensity is highly sensitive to numerous factors such as subject head anatomy, coil positioning, coil configuration, etc., iterative computer simulation is required to determine the desired electric field intensity inside the brain

This article has been accepted for publication in a future issue of this journal, but has not been fully edited. Content may change prior to final publication. Citation information: DOI 10.1109/ACCESS.2021.3112612, IEEE Access

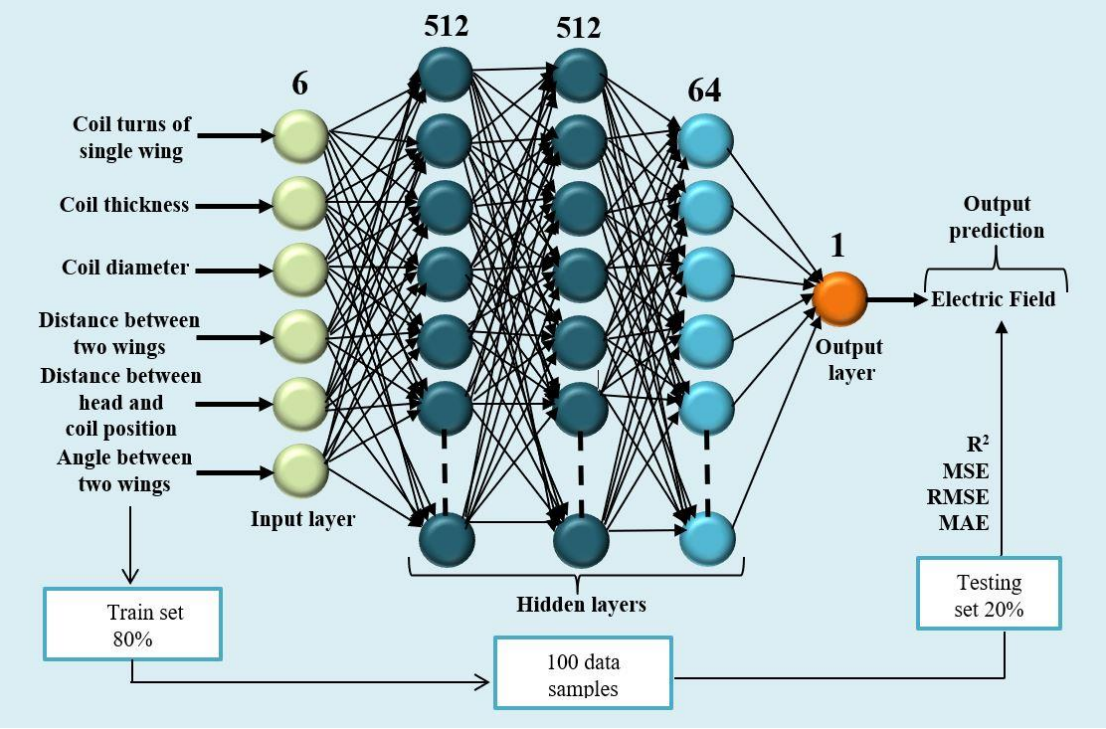

FIGURE 1. System architecture of proposed DNN based model for electric field prediction.

tissues. However, the problem associated with the electric field enumeration is that the computational time is generally high for the commercial electromagnetic (EM) simulation software [11, 12]. Moreover, the computational time is related to the development of a human head model and the estimation of the electric field with the aid of a volume conductor model [13, 14]. The important bottleneck is that it takes few hours to half a day to design a TMS coil on a human head model as well as to compute the electric field.

Therefore, the application of the deep learning (DL) approach could effectively resolve the computational cost issue [15]. Generally, the DL approach uses a layered structure of algorithm called artificial neural network (ANN) to solve several problems such as classification [16-19], regression [20-22], clustering [23, 24], and prediction [25-27]. Another advanced technique over shallow ANN called deep neural network (DNN) can develop a complex non-linear relationship with higher generalization capability by employing multiple hidden layers between the input and output [28] to compute optimum induced electric field.

Recently, very few researches have been reported to compute induced electric field of TMS coil in head model through DNN model. For example, Yokota et al. [11] proposed a DNN model to estimate the electric field of TMS coil in head MR images at different coil positions. They created datasets with the help of SimNIBS and FreeSurfer segmentation softwares to train and test the U-Net DNN model. The FreeSurfer software converted the MR image into a 3D head model and the SimNIBS software calculated the electric fields by the finite element method at varying positions of the figure-eight coil. Thereafter, the DNN model was trained with created datasets for mapping the electric field to the MR images. In another work, Afuwape et al. [12] utilized a deep learning method to predict electric field into T1-weighted MR images with varying coil configuration. The 3D head model was generated from the MR image and the finite element analysis was performed in Sim4Life software for sixteen different coil configurations. Then the deep convolutional neural network was trained using the generated dataset to predict the electric field of TMS coils in 3D head model.

Both of the models could estimate the electric field accurately within a short time. However, the segmentation process (3D head model generation) is time-consuming as well as complicated due to the generation of both brain and skull parts. It is also quite challenging to develop an accurate head structure from low contrast MR images. Besides segmentation time, both models take a longer training time to process the data with the deep network architecture. Moreover, the estimation of the electric field is done based on the single coil and single design parameter of coil positioning. Since, the induced electric field value is dependent on different coil designing parameters such as the coil turns, coil thickness, coil angle, coil diameter, etc. [29], the optimum field calculation based on these parameters is essential for a safe and effective TMS treatment. Moreover, the advantages associated with the tradeoff between focality and depth of induced electric field cannot be achieved by the single stimulation coil but can be achieved by assembly coil. Thereby, in this work a simple DNN approach is proposed for the prediction of electric field induced by TMS assembly coil, which directly regresses

This article has been accepted for publication in a future issue of this journal, but has not been fully edited. Content may change prior to final publication. Citation information: DOI 10.1109/ACCESS.2021.3112612, IEEE Access

electric field from six different coil designing parameters. This is a numerical data-driven method for predicting electric fields where the mapping of coil modeling parameters to the electric fields is achieved using a training dataset consisting of pairs of design parameters and the relative electric fields. The mapping is characterized by the model that consist of three non-linear hidden layers between the input and output layers. For the regression task, the model is trained with 100 data samples of six coil design parameters and electric field pairs. After training the deep neural network, the electric field induced by the transcranial magnetic stimulation coil is predicted directly from any TMS coil design parameter. The advantage related to the computation time is that the proposed DNN model requires only 0.04 s of time for computation using a graphics processing unit (GPU). This time is significantly lower compared to the conventional simulation software for the determination of the electric field induced by the TMS coil.

The primary contributions of this work are outlined as follows:

• A DNN approach as a nonlinear regression model to predict the induced electric field value from assembly TMS coil under high-valued and low-frequency current pulse conditions is proposed.

• The data normalization process is used for the input dataset before feeding to the proposed DNN model to arrange different valued input features into a similar format.

• The (6-512-512-64-1) DNN is modeled with a total of 1095 neurons for learning the complex behaviors of coil designing parameters and corresponding induced electric field from the input and output datasets.

• The performance of the proposed model is evaluated by analyzing the four regression matrices to predict the electric field from the assembly TMS coil.

The residual part of the paper is organized as follows: Section II presents the detailed explanation of the proposed methodology. The result is described in detail with some performance measures in Section III. Discussion and comparison with the existing works are done in Section IV. The conclusion and future directions of the paper are drawn in Section V.

II. PROPOSED APPROACH

The system architecture of the proposed DNN based prediction model is shown in FIGURE 1. The input and output of the proposed DNN model are the coil design parameters and the induced electric field respectively. The inner configuration of the DNN model with three non-linear hidden layers build a complex relationship between input parameters and output electric field. FIGURE 2 illustrates the workflow diagram of the overall process of the electric field prediction induced by the HVA TMS coil. In which the prediction process starts with the collection of data samples $(h, [\boldsymbol{x}_1; \boldsymbol{x}_2; \ldots; \boldsymbol{x}_6], \boldsymbol{E}) \in D$ from the mathematical model consisting of head anatomy, h, coil design parameters $[\boldsymbol{x}_1; \boldsymbol{x}_2; \ldots; \boldsymbol{x}_6]$ and its corresponding induced electric fields, $\boldsymbol{E}$. Then the preprocessing technique is performed just before splitting the dataset into a train, D_{train} and test, D_{test} sets. After that, the proposed DNN based regression model with the setting of optimal hyperparameters values is introduced for supervised learning using the training dataset. Finally, the electric field prediction, E_{pred} is performed using the test data on the trained DNN model with the evaluation of reasonable values of performance matrices. The details of the electric field prediction steps are described in the subsections below.

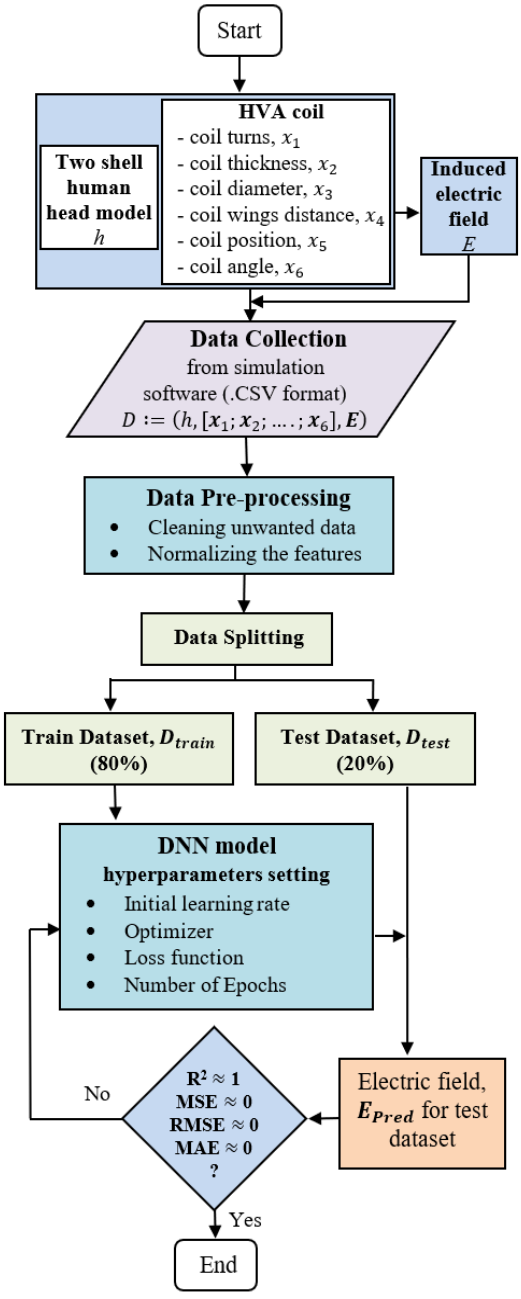

FIGURE 2. Flow diagram of DNN based electric field prediction process.

A. GEOMETRIC STRUCTURE OF HVA COIL WITH TWO SHELL HUMAN HEAD MODEL

FIGURE 3 illustrates the cross-section of the two-shell human head model with a halo-V assembly (HVA) coil

This article has been accepted for publication in a future issue of this journal, but has not been fully edited. Content may change prior to final publication. Citation information: DOI 10.1109/ACCESS.2021.3112612, IEEE Access

configuration. The head model is comprised of two different anatomical layers including the skull and tissue fluid. Both layers are indicated in the inset of the three-dimensional head model in the Cartesian coordinates system. The outer and inner radius of the skull structure are 85 mm and 80 mm respectively, while the inner part of the skull i.e., the fluid tissue region is modeled with a radius of 80 mm. The HVA stimulation coil consists of two coils including halo coil and V coil. These two coils have a different number of turns such as: 9 for both wings of the V coil and 5 for the halo coil which makes a total of 23 turns. The V coil part of the HVA coil is placed at a distance of 5 mm from the vertex of the head model. Similarly, the halo coil part is placed at 90mm from the vertex of the head model. The design parameters of the HVA coil are summarized in Table 1. Each of the coils is modeled by considering the torus shape of copper material with an electrical conductivity of 5.8×10^7 S/m. The electromagnetic properties of materials implicated in this model are listed in Table 2 [30, 31]. For coil excitation, a current pulse with the high amplitude of 5000A and low-frequency of 2500 Hz are applied in the coil domain.

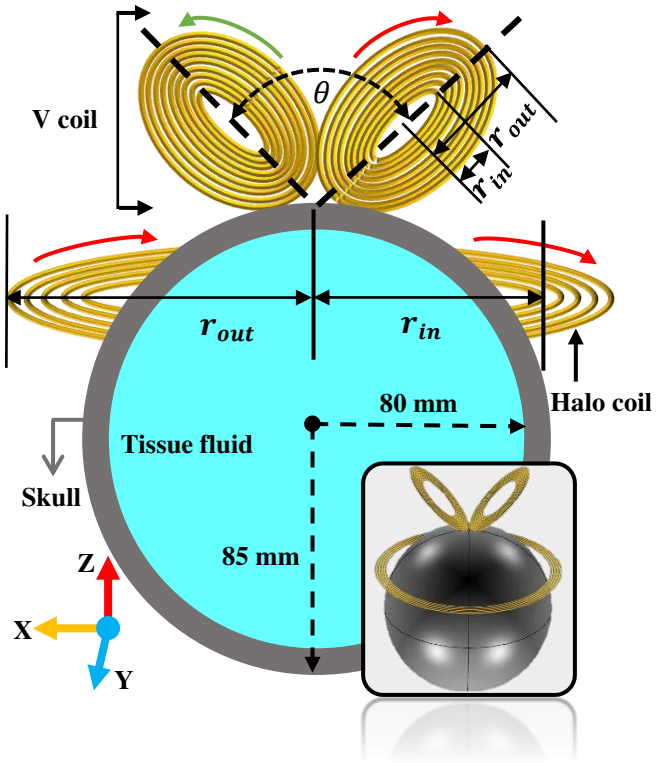

FIGURE 3. Configuration of HVA coil. The red and green arrow lines indicate the clockwise and anti-clockwise current direction respectively.

TABLE 1. Geometrical parameters of the HVA coil.

Coil name		Inner radius r_{in} (mm)	Outer radius r_{out} (mm)	Total coil turns	Angle between two wings θ (degree)
HVA	V	27.5	47.5	18	45^0
	Halo	87.5	97.5	5	-

The electric field generation by the HVA coil follows Maxwell's fourth equation of ampere's laws. The distribution of the charge carrier in the closed-loop coil generates a magnetic field in the direction perpendicular to the coil surface. As a result, the changing magnetic field induces an electric field in the conductive head tissue medium. Equations (1) to (4) presented in differential form are used to represent the generated magnetic field and induced electric field [32]. Here, J and J_e represent the current density vector and the externally generated current density respectively. The magnetic potential and intensity vector are indicated by A and B. Moreover, the induced electric field intensity and displacement vector are denoted as E and D respectively.

$$J = \sigma E + j\omega D + J_e \quad (1)$$

$$E = -\nabla V - j\omega A \quad (2)$$

$$\mathrm{B} = \nabla \times A \quad (3)$$

$$\mathrm{D} = \epsilon_0 \epsilon_r E \quad (4)$$

Based on the above equations the electric field intensity value is evaluated in COMSOL Multiphysics 5.0a software. In the simulation, the total model domain including head and coil geometries are divided into several sub-domains for solving the governing equations [33]. The free tetrahedral meshing elements are considered for simulation that ensures an effective numerical accuracy in a low computational time.

TABLE 2. Electromagnetic properties of coil material and anatomical layers at an operating frequency of 2500Hz.

Material	Conductivity [S/m]	Relative permittivity	Relative permeability
Skull	0.02	30380	1
Tissue fluid	4	80	0.99
Copper	5.8×10^7	1	0.99

TABLE 3. Interpretation of input and output features.

Inputs and outputs	Features to form model (unit)	Range
Input	Coil turns of single wing	1-15
	Coil thickness (mm)	0.1-0.9
	Coil diameter (mm)	60-110
	Distance between two wings (mm)	0.5-10
	Distance between head and coil position (mm)	1-15
	Angle between two wings (degree)	5-90
Output	Electric field (v/m)	130-300

B. DATASET CREATION

For two shell head model (h), the electric fields, E_n are computed for six different parameters of HVA coil including coil turns of single wing (x_1), coil thickness (x_2), coil diameter (x_3), distance between two wings (x_4), distance between head and coil position (x_5), and angle between two wings (x_6). The variation of the values of each input parameter are summarized in Table 3. The dataset is obtained

This article has been accepted for publication in a future issue of this journal, but has not been fully edited. Content may change prior to final publication. Citation information: DOI 10.1109/ACCESS.2021.3112612, IEEE Access

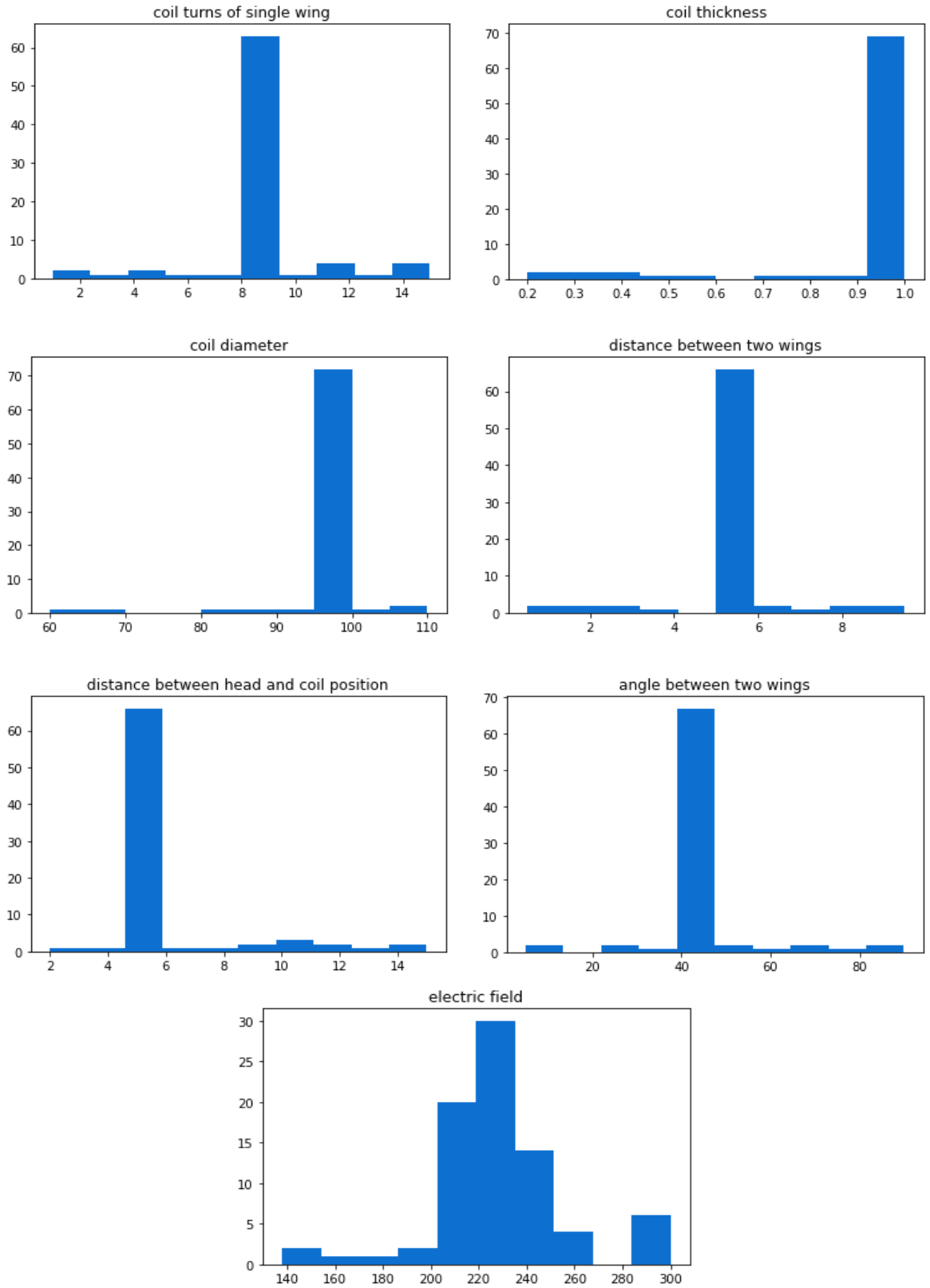

FIGURE 4. Histogram for original feature visualization.

This article has been accepted for publication in a future issue of this journal, but has not been fully edited. Content may change prior to final publication. Citation information: DOI 10.1109/ACCESS.2021.3112612, IEEE Access

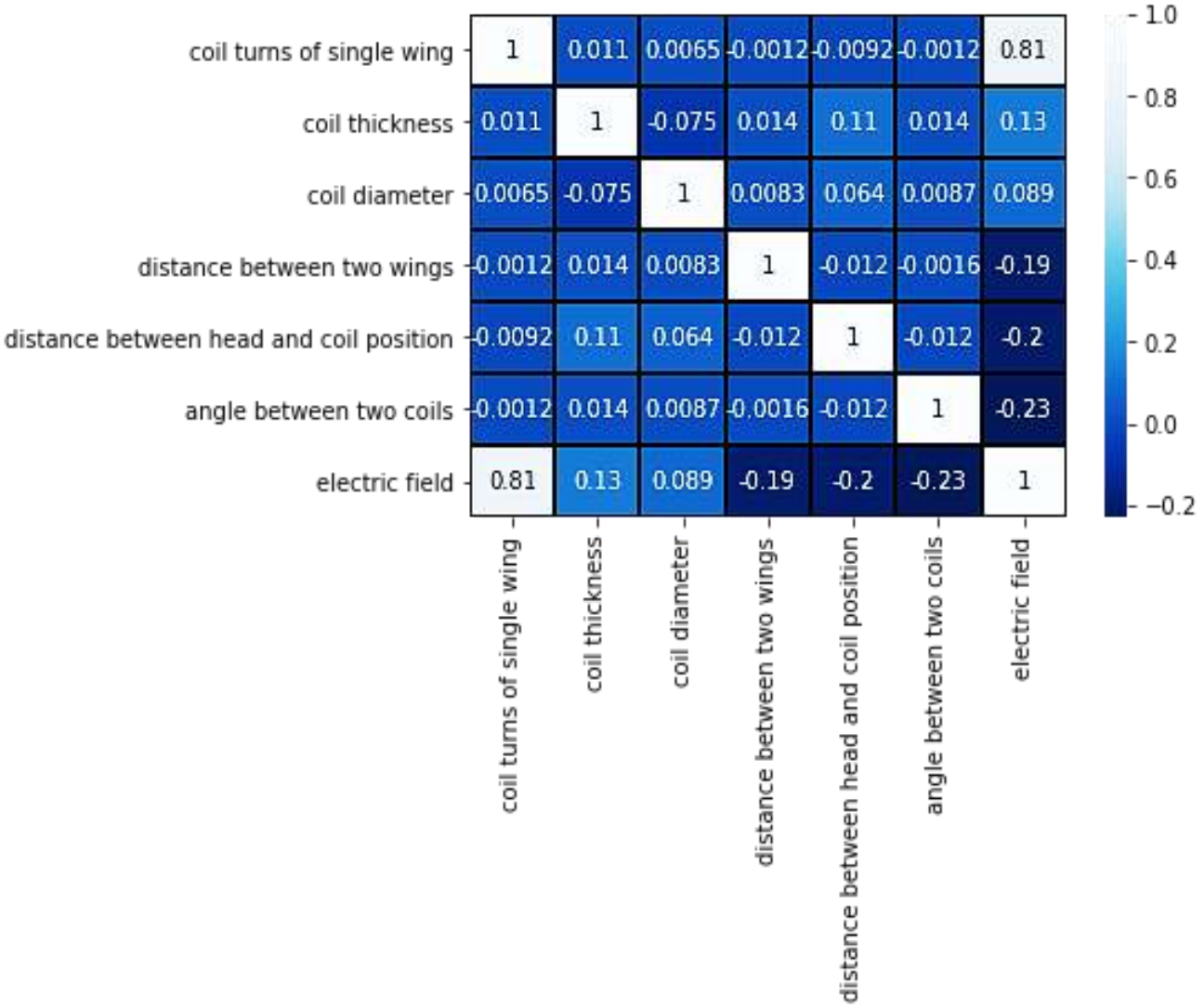

FIGURE 5. **Correlation matrix heatmap of attributes.**

by setting D: = $\{h, [x_1; x_2; \ldots; x_6]_n, E_n\}_{n=1}^{N}$ with a total of N=100 samples. Here, $\{E_n\}_{n=1}^{N}$ is found from $\{h, [x_1; x_2; \ldots; x_6]_n\}_{n=1}^{N}$ under the low frequency of 2500Hz and high amplitude of 5000A current pulse conditions. All the data samples are collected from COMSOL Multiphysics software in .csv format for the processing with the proposed DNN model.

C. DATA PRE-PROCESSING

Data preprocessing is an important part to increase the model prediction accuracy. This section gives a technical specification of the data preprocessing steps for our proposed prediction model. Moreover, the statistical analysis is conducted for a better understanding of the dataset, cleaning unwanted data, normalizing the features, and spliting the dataset. The histogram plots of features are shown in FIGURE 4 to understand the distribution of each attribute independently. Among all input features, the coil thickness and coil diameter are negatively skewed and they have a

TABLE 4. **Statistical values of input and output features.**

Features	Mean	Standard Deviation	Min	Max
Coil turns of single wing	9.02	2.16	1.00	15.00
Coil thickness	0.93	0.19	0.20	1.00
Coil diameter	94.18	5.93	60.00	110.00
Distance between two wings	4.99	1.32	0.50	9.50
Distance between head and coil position	5.81	2.32	2.00	15.00
Angle between two wings	45.94	11.08	5.00	90.00
Electric field	229.87	31.26	138.00	329.00

This article has been accepted for publication in a future issue of this journal, but has not been fully edited. Content may change prior to final publication. Citation information: DOI 10.1109/ACCESS.2021.3112612, IEEE Access

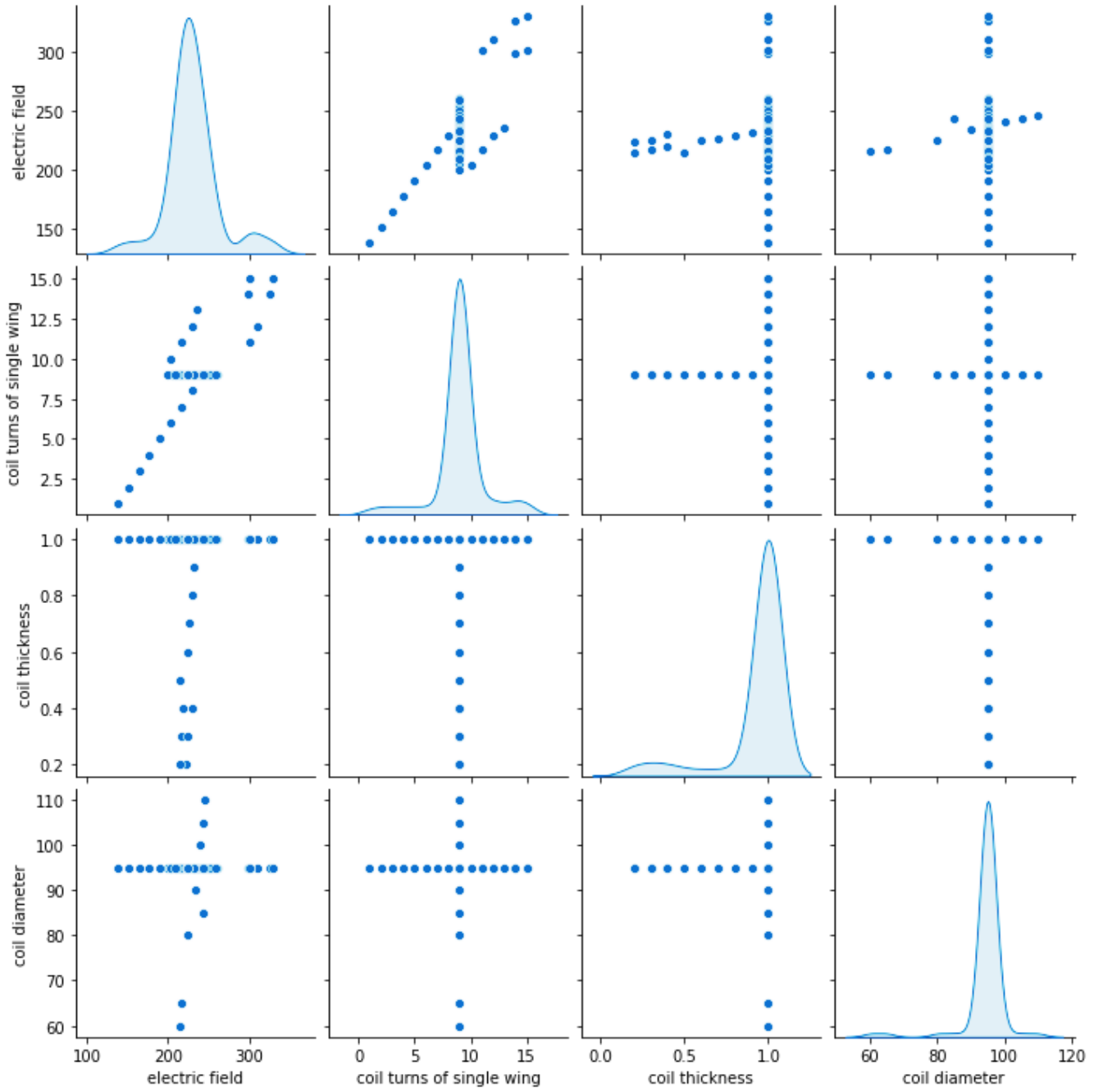

FIGURE 6. Scatterplot matrix of features.

great impact on the prediction model. The correlation between two quantitative attributes is visualized based on the correlation matrix heatmap as shown in FIGURE 5. Analysis of correlation matrix provides six important unique input features such as coil turns of single wing, coil thickness, coil diameter, distance between two wings, distance between head and coil position, and angle between two wings of coil that are more correlated with the outputs feature of electric field. FIGURE 5 indicates that the strong relationship between the attributes gives a high correlation value whereas hardly related attributes provide low correlation value. Moreover, the scatterplot matrix shown in FIGURE 6 provides information about the structured relationship between the attributes. From the first row of the scatter plot matrix, it is obvious that the scatter plot of the output electric field is the function of all input features. Similarly, each input feature is the function of the output electric field as presented in other rows. The join distributions of three input features (i.e., coil turns of the single wing, coil thickness, coil diameter) and output feature (i.e., electric field) are shown diagonally in the scatterplot matrix. The statistical analyzes

This article has been accepted for publication in a future issue of this journal, but has not been fully edited. Content may change prior to final publication. Citation information: DOI 10.1109/ACCESS.2021.3112612, IEEE Access

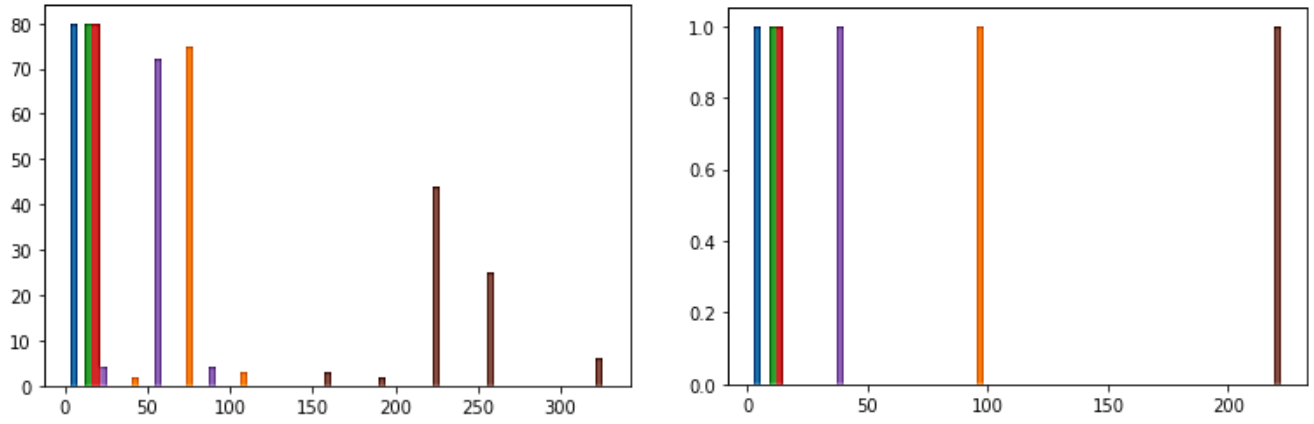

(a) Original input features with numeric value.

(b) Input features after normalization.

FIGURE 7. Numeric input feature and its normalization.

based on mean, standard deviation, minimum, and maximum values are conducted to examine the feature-wise values that are summarized in Table 4. From this table, it is seen that the range of each feature is different from others. The minimum and maximum ranges of all features are set to a considerable value to remove bad working points. All the input and output features in the dataset are in numeric forms as continuous measurement data. Consequently, the normalization technique is applied for numeric features prior to training the proposed DNN model. The normalization technique coerces the values of all features into a distribution centered around 0 with a standard deviation of 1 by precomputing the mean and variance of the features as shown in Table 4. The numeric original feature and the corresponding normalized features are depicted in FIGURE 7.

D. PROPOSED DNN MODEL

In a DNN model, the number of nodes in hidden input and output layers are identical to the numbers of input and output features [34]. However, the number of nodes and hidden layers can be varied depending on the complexity of the problem and the data set. The proposed DNN model architecture as shown in FIGURE 8 comprises of an input layer with six nodes, three fully connected (dense) hidden layers with 512-512-64 nodes for the first, second, and third layers respectively, and an output dense layer with one node for the prediction of electric field, E_{pred}. The electric field value can be calculated by using equation (5) as:

$$E_{pred} = Linear\left[ReLU_{1,2,3\in h}\left(\begin{bmatrix} x_1 \\ x_2 \\ \vdots \\ x_6 \end{bmatrix} \bullet W_{i,j}^{(k)} + b_i^{(k)}\right)\right] \quad (5)$$

where $W_{i,j}^{(k)}$ is the weight connecting to the *i*th unit in *k*th hidden layer and *j*th unit of previous layer, and $b_i^{(k)}$ is the bias connecting the *i*th unit in the *k*th hidden layer. A non-linear transfer function called rectified linear unit (ReLU) is selected for the hidden layers that provides a non-linearity to the DNN regression model. ReLU is defined as:

$$ReLU\,(P_h) = \max\,(0, P_h) \quad (6)$$

Where,

$$P_h = \begin{bmatrix} x_1 \\ x_2 \\ \vdots \\ x_6 \end{bmatrix} \bullet W_{i,j}^{(k)} + b_i^{(k)} \quad (7)$$

A linear transfer function is also assigned for the output layer to predict the single electric field value. The mean absolute error loss function is chosen for the model to determine the optimum values of trainable parameters such as weight, $W_{i,j}^{(k)}$ and bias, $b_i^{(k)}$. Then, the Adam optimizer is selected with a default learning rate of 0.001 to minimize the loss function [35]. The optimizer minimizes the loss function by updating the trainable parameters with its gradients that are found by the backpropagation method. The entire dataset used for the model is divided into two sets with an amount of 80% for the training, and the residual 20% for testing.

III. RESULTS

In this work, the 6-512-512-64-1 DNN model with 299,150 trainable parameters achieve the best performance for the purpose of electric field prediction. Table 5 summarizes the results of four verification matrices such as coefficient of determination (R^2), mean squared error (MSE), mean absolute error (MAE), and root mean squared error (RMSE), which are commonly used to analyze the model prediction. Equations (8) to (12) are employed to define the four above-mentioned metrics. Here, y_{true} indicates the true output, y_{pred} indicates the predicted output, and the mean of the ground truth output is represented as y_{mean}. The total number of data is denoted as n.

$$y_{mean} = \frac{1}{n}\sum_{k=1}^{n} y_{true} \quad (8)$$

This article has been accepted for publication in a future issue of this journal, but has not been fully edited. Content may change prior to final publication. Citation information: DOI 10.1109/ACCESS.2021.3112612, IEEE Access

$$R^2 = 1 - \frac{\sum_{k=1}^{n}(y_{true} - y_{pred})^2}{\sum_{k=1}^{n}(y_{true} - y_{mean})^2} \in [0, 1] \quad (9)$$

$$MSE = \frac{\sum_{k=1}^{n}(y_{true} - y_{pred})^2}{n} \quad (10)$$

$$MAE = \frac{\sum_{k=1}^{n}|y_{true} - y_{pred}|}{n} \in [0, +\infty] \quad (11)$$

$$RMSE = \sqrt{\frac{\sum_{k=1}^{n}(y_{true} - y_{pred})^2}{n}} \in [0, +\infty] \quad (12)$$

Layer (type)	Output Shape	Param #
normalization	(None, 6)	13
dense (Dense)	(None, 512)	3584
dense (Dense)	(None, 512)	262656
dense (Dense)	(None, 64)	32832
dense (Dense)	(None, 1)	65

Total params: 299,150

FIGURE 8. Proposed DNN model architecture.

The R^2 metric represents the quality of the proposed DNN regression model. It determines how well the model predicts the electric field value. To perfectly fit the data of the regression prediction model, the value of R^2 is considered to be equal to 1. However, the regression loss function, MSE is calculated by summing the squared of distances between the true value and predicted value. The value of MSE=0 is preferable. Another loss function called MAE is measured by averaging all absolute errors. RMSE is also calculated by the square root of the sum of square deviation of true and predicted values over the total number of data n. For perfectly fitting the predicted values to the true values, the RMSE=0 is desirable.

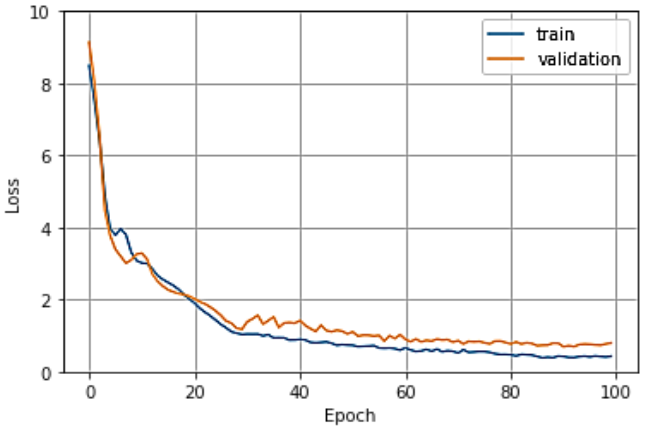

FIGURE 9. Loss versus epoch plot for the DNN model.

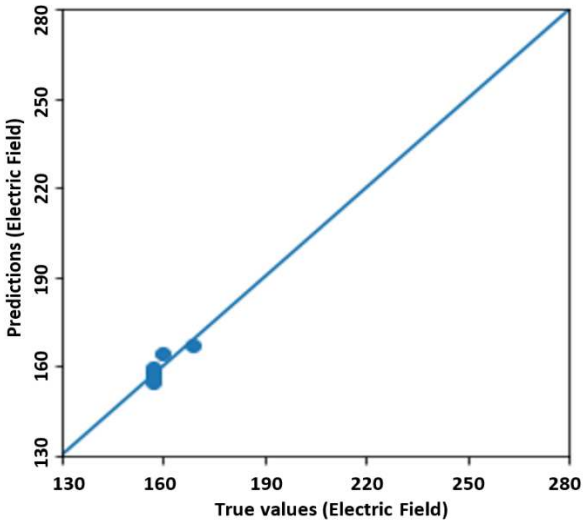

FIGURE 10. The predicted electric field values versus simulated data on test set.

The training process of the proposed DNN model against 100 iterations (epochs) is shown in FIGURE 9, in which the training and validation loss are found equal at 20 epochs. After 20 epochs, both errors are started to decrease at an optimum level and the finest result is achieved within the epochs of 90 to 100.

TABLE 5. Results of four verification matrices

R^2	MSE	MAE	RMSE
0.766	0.184	0.262	0.429

The predicted electric field values are plotted against true electric field values (simulated values) for the proposed model which is shown in FIGURE 10. The graph indicates that the prediction accuracy of the proposed DNN model is good enough as the predicted electric field values are quite similar to the simulated electric field values. Therefore, the proposed model has the capability to predict the electric field values ranging from 130 V/m to 300 V/m in an accurate manner. Moreover, the prediction accuracy of the model as a function of single input feature (i.e., coil turns of single wing) is shown in FIGURE 11. For a range of values of input feature, there is a considerable number of accurate predictions of the electric field values of the HVA TMS coil under high amplitude and low-frequency current conditions.

This article has been accepted for publication in a future issue of this journal, but has not been fully edited. Content may change prior to final publication. Citation information: DOI 10.1109/ACCESS.2021.3112612, IEEE Access

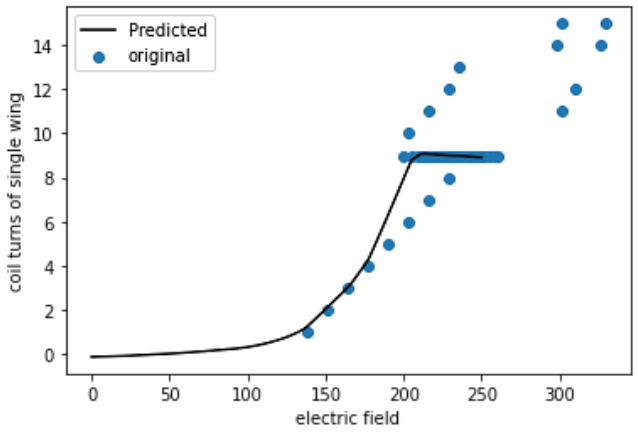

FIGURE 11. The predicted electric field values as a function of the single input feature of coil turns of single wing.

IV. DISCUSSION

The main advantage of the proposed DNN model is that it can estimate the induced electric field in a head model much faster way than the electric field determination process by an EM software. The electric field computational time for the proposed DNN model and simulation software are determined. Table 6 represents the computation time to estimate the induced electric field in a head model from a HVA TMS coil. The expected values of computation time using GPU and CPU for the proposed DNN model are found 0.04 s and 1.98 s respectively. On the other hand, the required computation time for COMSOL Multiphysics software is found 6 min 15 s even though this estimated time exclude the construction time of anatomical head and coil model. If the construction time of anatomical head and coil model is considered then it will be few hours.

TABLE 6. Computation time to estimate electric field for HVA TMS coil.

Model	Computation time
DNN (GPU)	0.04 s
DNN (CPU)	1.98 s
Simulation software (Excluding coil and anatomical head modeling)	6 min 15 s

Moreover, the performance comparison of the proposed DNN based approach with the couple of similar state-of-the-art approaches is presented in Table 7. The works reported in in [11-12] also used DNN model to estimate electric field but they used single coil and single coil parameter to determine electric field. Single coil is not suitable for the trade-off between stimulation focality and depth [10]. For getting optimal treatment efficacy and minimal side effect, focality and depth trade-off is essential. Thus, DNN based electric field estimation for assembly coil with multiple coil parameters is done in this work. Table 7 indicate than that the proposed model can predict electric field for several coil parameters at a bit lower R^2 value. However, the lower value of R^2 in compare to the existing works is found because of the lower number of training datasets used. The value of R^2 can be improved by employing several data increment methods. Since, the use of an assembly coil rather than a single coil can provide optimum therapeutic support to the neural disorder patient, the optimum electric field determined from an assembly coil for varying coil parameters can provide an effective and safe stimulation during treatment against neurological disorders.

TABLE 7. Comparison between the proposed model and existing related works.

Reference	[11]	[12]	This work
Prediction model	U-Net	Deep CNN	DNN
Data type	Image	Image	Numerical value
Total dataset	261,072	800	100
Coil type	single	single	assembly
Coil parameter	coil position	-	. coil position . coil turns . coil thickness . coil diameter . coil angle . coil wings distance
Performance evaluation matrix	CC=0.93 PSNR= 29dB MAE=6 RMAD=6%	R^2 = 0.92 MAPE = 6.2%	R^2 = 0.766 MSE = 0.184 MAE = 0.262 RMSE = 0.429

V. CONCLUSION

This paper introduces a DNN based regression model for predicting electric field induced by HVA transcranial magnetic stimulation coil inside a head model. The database uses for training the DNN model consists of 100 simulated data. These 100 data are obtained for different coil parameters. The model exhibits reasonable prediction accuracy of $R^2 = 0.766$ which ensures the ability of the model to predict electric field for HVA coil with varied parameters. Moreover, the model can efficiently estimate electric field in a very short time of 0.04 s without any requirement of the mathematical or three-dimensional model for human head phantom and TMS coil. Thus, the proposed DNN model can effectively reduce the electric field computation cost and help manufacturer to build an optimum coil for the treatment of the certain neurological disorder. In future, data augmentation process can be used to increase the number of datasets and to reduce the overfitting problems related to the model. Moreover, the critical stimulation parameters including focality and depth can also be considered as the predictive values to reduce the possibility of undesired side effect with the aid of other optimization algorithms including differential evolution, genetic algorithm, particle swarm optimization, etc.

REFERENCES

[1] F. Spagnolo *et al.*, "Bilateral Repetitive Transcranial Magnetic Stimulation With the H-Coil in Parkinson's Disease: A Randomized, Sham-Controlled Study," *Frontiers in neurology,* vol. 11, p. 1831, 2021.

[2] G. Schiena, E. Maggioni, S. Pozzoli, and P. Brambilla, "Transcranial magnetic stimulation in major depressive disorder: Response modulation and state dependency," *Journal of affective disorders,* vol. 266, pp. 793-801, 2020.

[3] T. Bender Pape *et al.*, "Safety considerations for the use of transcranial magnetic stimulation as treatment for coma recovery in people with severe traumatic brain injury," *Journal of Head Trauma Rehabilitation,* vol. 35, no. 6, pp. 430-438, 2020.

[4] M. Isserles *et al.*, "Deep Transcranial Magnetic Stimulation Combined with Brief Exposure for Post-Traumatic Stress Disorder–A Prospective Multisite Randomized Trial," *Biological Psychiatry,* 2021.

[5] O. Afuwape, P. Rastogi, and D. Jiles, "Comparison of the Effect of Coil Configuration and the Variability of Anatomical Structure on Transcranial Magnetic Stimulation," *IEEE Transactions on Magnetics,* 2020.

[6] M. Lu and S. Ueno, "Comparison of the induced fields using different coil configurations during deep transcranial magnetic stimulation," *PloS one,* vol. 12, no. 6, p. e0178422, 2017.

[7] T. Pashut *et al.*, "Mechanisms of magnetic stimulation of central nervous system neurons," *PLoS Comput Biol,* vol. 7, no. 3, p. e1002022, 2011.

[8] J. C. Lin, "Transcranial Magnetic Stimulation Therapy for Depression and Psychiatric Disorders [Health Matters]," *IEEE Microwave Magazine,* vol. 17, no. 8, pp. 23-93, 2016.

[9] S. Rossi, M. Hallett, P. M. Rossini, A. Pascual-Leone, and S. o. T. C. Group, "Safety, ethical considerations, and application guidelines for the use of transcranial magnetic stimulation in clinical practice and research," *Clinical neurophysiology,* vol. 120, no. 12, pp. 2008-2039, 2009.

[10] L. I. N. de Lara *et al.*, "A 3-axis coil design for multichannel TMS arrays," *NeuroImage,* vol. 224, p. 117355, 2021.

[11] T. Yokota *et al.*, "Real-time estimation of electric fields induced by transcranial magnetic stimulation with deep neural networks," *Brain stimulation,* vol. 12, no. 6, pp. 1500-1507, 2019.

[12] O. F. Afuwape, O. O. Olafasakin, and D. C. Jiles, "Neural Network Model for Estimation of the Induced Electric Field during Transcranial Magnetic Stimulation," *IEEE Transactions on Magnetics,* 2021.

[13] A. Kybartaite, "Computational representation of a realistic head and brain volume conductor model: electroencephalography simulation and visualization study," *International journal for numerical methods in biomedical engineering,* vol. 28, no. 11, pp. 1144-1155, 2012.

[14] M. Fuchs, M. Wagner, and J. Kastner, "Development of volume conductor and source models to localize epileptic foci," *Journal of Clinical Neurophysiology,* vol. 24, no. 2, pp. 101-119, 2007.

[15] E. A. Rashed, J. Gomez-Tames, and A. Hirata, "Deep learning-based development of personalized human head model with non-uniform conductivity for brain stimulation," *IEEE transactions on medical imaging,* vol. 39, no. 7, pp. 2351-2362, 2020.

[16] E. Dandıl, M. Çakiroğlu, Z. Ekşi, M. Özkan, Ö. K. Kurt, and A. Canan, "Artificial neural network-based classification system for lung nodules on computed tomography scans," in *2014 6th International conference of soft computing and pattern recognition (SoCPaR)*, 2014, pp. 382-386: IEEE.

[17] F. Shaukat, G. Raja, R. Ashraf, S. Khalid, M. Ahmad, and A. Ali, "Artificial neural network based classification of lung nodules in CT images using intensity, shape and texture features," *Journal of Ambient Intelligence and Humanized Computing,* vol. 10, no. 10, pp. 4135-4149, 2019.

[18] V. A. Maksimenko *et al.*, "Artificial neural network classification of motor-related eeg: An increase in classification accuracy by reducing signal complexity," *Complexity,* vol. 2018, 2018.

[19] Z. Cömert and A. F. Kocamaz, "A study of artificial neural network training algorithms for classification of cardiotocography signals," *Bitlis Eren University journal of science and technology,* vol. 7, no. 2, pp. 93-103, 2017.

[20] M. Bataineh and T. Marler, "Neural network for regression problems with reduced training sets," *Neural networks,* vol. 95, pp. 1-9, 2017.

[21] I. I. Argatov and Y. S. Chai, "An artificial neural network supported regression model for wear rate," *Tribology International,* vol. 138, pp. 211-214, 2019.

[22] D. F. Specht, "A general regression neural network," *IEEE transactions on neural networks,* vol. 2, no. 6, pp. 568-576, 1991.

[23] Y. Raptodimos and I. Lazakis, "Using artificial neural network-self-organising map for data clustering of marine engine condition monitoring applications," *Ships and Offshore Structures,* vol. 13, no. 6, pp. 649-656, 2018.

[24] E. Sharghi, V. Nourania, A. AliAshrafia, and H. Gökçekuşb, "Monitoring effluent quality of wastewater treatment plant by clustering based artificial neural network method," *Desalination and Water Treatment,* vol. 164, pp. 86-97, 2019.

[25] M. Matos, S. Pinho, and V. Tagarielli, "Predictions of the electrical conductivity of composites of polymers and carbon nanotubes by an artificial neural network," *Scripta Materialia,* vol. 166, pp. 117-121, 2019.

[26] Y. L. Zhukovskiy, N. Korolev, I. Babanova, and A. Boikov, "The prediction of the residual life of electromechanical equipment based on the artificial neural network," in *IOP Conference Series: Earth and Environmental Science*, 2017, vol. 87, no. 3, p. 032056: IOP Publishing.

[27] F. Mohamadian, L. Eftekhar, and Y. Haghighi Bardineh, "Applying GMDH artificial neural network to predict dynamic viscosity of an antimicrobial nanofluid," *Nanomedicine Journal,* vol. 5, no. 4, pp. 217-221, 2018.

[28] Z. An, S. Li, J. Wang, Y. Xin, and K. Xu, "Generalization of deep neural network for bearing fault diagnosis under different working conditions using multiple kernel method," *Neurocomputing,* vol. 352, pp. 42-53, 2019.

[29] S. Zibman, G. S. Pell, N. Barnea-Ygael, Y. Roth, and A. Zangen, "Application of transcranial magnetic stimulation for major depression: coil design and neuroanatomical variability considerations," *European Neuropsychopharmacology,* 2019.

[30] P. V. H. e. al., "Dipole localization errors due to not incorporating compartments with anisotropic conductivities: Simulation study in a spherical head model," *Int. J. Biolelectromagnetism,* vol. 7, pp. 134-137, 2005.

[31] C. Gabriel, *Complication of the dielectric properties of body tissues at RF and microwave frequencies*. Dept. Phys., King's College London, London, U.K., Brooks Air Force Tech. Rep. AL/OE-TR-1996-0004, 1996.

[32] Y.-Y. Tsai, "TMS Coil Design," *Bachelor thesis. Worchester Polytechnic Institute,* 2011.

[33] A. L. Benabid, S. Chabardes, J. Mitrofanis, and P. Pollak, "Deep brain stimulation of the subthalamic nucleus for the treatment of Parkinson's disease," *The Lancet Neurology,* vol. 8, no. 1, pp. 67-81, 2009.

[34] W. Liu, Z. Wang, X. Liu, N. Zeng, Y. Liu, and F. E. Alsaadi, "A survey of deep neural network architectures and their applications," *Neurocomputing,* vol. 234, pp. 11-26, 2017.

[35] D. P. Kingma and J. Ba, "Adam: A method for stochastic optimization," *arXiv preprint arXiv:1412.6980,* 2014.

This article has been accepted for publication in a future issue of this journal, but has not been fully edited. Content may change prior to final publication. Citation information: DOI 10.1109/ACCESS.2021.3112612, IEEE Access

KHALEDA AKHTER SATHI received the B.Sc. degree in electronics and telecommunication engineering (ETE) from the Rajshahi University of Engineering and Technology (RUET), Rajshahi, Bangladesh, in 2019. She is currently working as a Lecturer with the Department of ETE, CUET. Her research interests include brain stimulation, medical image processing, and deep learning.

MD. AZAD HOSSAIN (Member, IEEE) received his B.Sc. degree from the Department of Electrical and Electronic Engineering, Rajshahi University of Engineering and Technology (RUET), in 2004 and M.Sc. and Ph.D. in 2010 and 2013, respectively, from Saga University, Saga, Japan. He is currently serving as Associate Professor with the Department of Electronics and Telecommunication Engineering in Chittagong University of Engineering & Technology, CUET. His research interests include antenna for polarization switching and detection, antenna for biomedical application, Brain stimulation, RF energy harvesting, 5G antenna and MIMO antenna design. He is the member of IEEE.

MD. KAMAL HOSAIN received his PhD from the School of Engineering at Deakin University, Australia. He received his BSc in Electronics and Communication Engineering from Khulna University of Engineering & Technology, Bangladesh in 2006. He is currently working as a Professor in the Department of Electronics & Telecommunication Engineering, Rajshahi University of Engineering & Technology, Bangladesh. Dr. Hosain has been working in the area of Antenna and Biomedical Engineering for last ten years and he has published a number of research papers in this field. He is a member of Institute of Engineers Bangladesh (IEB). His research interests include development of miniature electronic devices, brain stimulation, antennas and its application in brain stimulation, design and analysis of power electronic devices, modelling and simulation of biosensors, etc. Dr. Hosain, with his dedicated research team, is looking forward to explore brain stimulation and antennas in biomedical applications through extensive research and analysis of various stimulation parameters, devices, antenna parameters, bio-compatibility, etc.

NGUYEN HOANG HAI (Member, IEEE) was born in Hanoi, Vietnam, in 1977. He received the B.E. degree in electronics and telecommunication engineering from the Hanoi University of Technology (HUT) in 1999, the Ph.D. degree in in electrical and electronics engineering from the University of the Ryukyus, Okinawa, Japan, in 2009, In October 2000, he joined the Department of Electrical and Electronics Engineering, University of the Ryukyus, as a Graduate Student, where he worked in the field of microwave circuit elements, electromagnetic theory. He is currently pursuing the Ph.D. degree with the Department of Electrical and Electronics Engineering, University of the Ryukyus. After completion of his Ph.D. degree, he joined the Department of Telecommunication System, School of Electronics and Telecommunication, Hanoi University of Science and Technology in 2009. In 2013, he became an Associate Professor with the Department of Telecommunication System, School of Electronics and Telecommunication, HUST, where he became an Associate Professor in 2013. He became a Deputy Head of the Department of Telecommunication System in 2013. He has been engaged in research on analysis of optical fiber transmission characteristics, chromatic dispersion (CD), polarization characteristics, polarization mode dispersion (PMD), and highly nonlinear effect in optical system, in single mode optical fibers and optical fiber submarine system. Recently, he focuses research on optimized designs for various types of photonic crystal fibers (PCFs) and its application for broadband transmission system, and medical application as well.

MD. ANWAR HOSSAIN (Senior Member, IEEE) received the B.Sc. (Engineering) degree in electrical and electronic engineering from the Rajshahi University of Engineering and Technology, Rajshahi, Bangladesh, in 2001, the M.E. degree in information and communication technology from the Asian Institute of Technology Pathumthani, Thailand, in 2006, and the Ph.D. degree in electronics and information engineering under interdisciplinary intelligent systems engineering from the University of the Ryukyus, Nishihara, Japan, in 2013. He is currently working as a Professor with the Electrical and Electronic Engineering Department, Bangladesh University of Business and Technology (BUBT), Dhaka, Bangladesh. He is also doing research with the Electrical and Electronic Engineering Department, Independent University, Bangladesh (IUB), School of Electronics and Telecommunications, Hanoi University of Science and Technology, Vietnam, and the University of the Ryukyus, Japan. His research interests include photonic sensors, biophotonics, photonic crystals fibers, optoelectronic devices and systems, antenna array signal processing (Beamforming), CDMA, optical CDMA, and OFDM. He received Postdoctoral Fellowship from the Japan Society for the Promotion of Science in 2015.